Scientific Research Publishing

Stability Analysis of Electromagnetic Ordinary and Extraordinary Modes

N. Noreen[1], S. Zaheer[1], H. A. Shah[2]

[1]Forman Christian College, Chartered University, Lahore, Pakistan
[2]Government College University, Lahore, Pakistan
Email: nailanoreen@fccollege.edu.pk

Abstract

By using kinetic theory, we derived the general dispersion relations for ordinary mode (O-mode) and Extra-ordinary mode (X-mode) in anisotropic magnetized plasma. The effects of energy anisotropy, magnetic field to density ratio (Ω_0/ω_p) and the plasma beta $\beta_\parallel$ on the propagation characteristics, have been analyzed. The stability analysis and the growth rates have been presented. The marginal threshold condition for oscillatory and purely growing mode has been obtained for higher harmonics and we have also calculated their growth rates in terms of plasma beta $\beta_\parallel$ and energy anisotropy $T_\perp/T_\parallel$. The X-mode satisfies the instability condition according to difference of geometry with the O-Mode. These modes are important for spherical tokamaks, and their coupling leads to the generation of the Bernstein mode, which causes the heating effects.

Keywords

1. Introduction

The ordinary mode (O-mode) is a linearly polarized electromagnetic perpendicularly propagating wave, which propagates only when wave frequency is greater than the plasma frequency. The work is related to the electromagnetic cyclotron harmonic instability for its possible role in solar and interplanetary radio emission processes where the ratio ω_p/Ω_0 (where ω_p is the electron plasma frequency and Ω_0 is the electron cyclotron frequency) is relatively high *i.e.*, the ratio is of the order of 10 or can be as high as 50 or even 100 near 1 a.u. It may be useful for the heating and current drive mechanism in the spherical tori like the NSTX [1] and MAST [2] where the $\omega_p > \Omega_0$.

It is found that extraordinary mode (X-mode) power is not absorbed at the cyclotron resonance but uniquely at the upper hybrid resonance, displaced to the low field side of the cyclotron resonance. O-mode power, however,

is absorbed at the cyclotron resonance as well. The displacement of the upper hybrid resonance to the low field side with O-mode launch is significantly smaller than that with X-mode launch because of the lower densities produced by O-mode launch at the same microwave power level [3]. Hamasaki [4] [5] investigated the electromagnetic o-mode instability with perpendicularly propagating waves for a two temperature Maxwellian distribution function. Lee [6] studied the same mode in counterstreaming plasmas and showed that the ordinary mode became unstable as the magnetic field changed. Later Bornatici and Lee [7] worked on O-mode and determined that for counterstreaming plasmas an instability occurred if the streaming velocity exceeded a certain threshold value which can be below the required velocity to excite the electrostatic two-stream instability. They also concluded that whereas the perpendicular temperature stabilized the effect the parallel temperature enhanced the instability. Shivamoggi [8] also discussed the destabilization of the O-mode due to magnetic field and thermal effects. Ibscher *et al.* [9] investigated the nonresonant Wieble mechanism which can drive the O-mode unstable. They studied the instability on the basis of a threshold which gave the instability conditions and upper limits of the growth rate. Their problem was restricted for fundamental harmonic only. Iqbal *et al.* [10] studied the O-mode in degenerate anisotropic plasmas and proposed the excitation of a new banded type of instability which grew at some particular values of temperature anisotropy. Hadi *et al.* [11] also revised the analysis of the O-mode instability with Maxwellian parallel distribution coupled with thermal ring perpendicular distribution. They demonstrated that O-mode for thermal ring distribution may be excited for cyclotron harmonics as well as for the purely growing branch, depending on the value of the normalized ring speed. Lazar *et al.* [12] concluded that O-mode instability was driven by an excess of parallel temperature where $A = \dfrac{T_\perp}{T_\parallel} < 1$

for $\beta_\parallel > 1$. Vafin *et al.* [13] derived the analytical marginal instability condition for magnetized plasmas when charged particles were distributed in counter-streams with equal temperatures. They confirmed the O-mode instability at small plasma beta values, when the parallel counter-stream free energy exceeded the perpendicular bi-Maxwellian free energy. Farrell [14] presented a theory in which he described the direct generation of electromagnetic O-mode emission via mildly energetic electron beams in a highly dense and warm plasma.

In this manuscript, the energy anisotropic Heaviside distribution function is used for understanding the behavior of O-mode and X-mode. Such distribution function provides the detailed information about banded emission of O-mode instability. Such type of emission has been observed in space plasmas, where $\omega_p / \Omega_0 > 10$ e.g. solar wind. Satellite wave instruments commonly detect banded magnetospheric emissions between harmonics of the electron gyrofrequency in the outer magnetosphere [15]. This type of banded emission has been observed in the terristial magnetosphere. Frequency-banded electromagnetic waves up to 2000 Hz are observed concurrently with warm energy-banded ions in the low latitude auroral and sub-auroral zones during every large geomagnetic storm, observed by the FAST and DEMETER satellites. The appearance of the banded wave activity suggests that there may be distinct changes in the geospace system that characterize large magnetic storms [16].

Coupling of the O-mode and X-mode is a necessary tool for generation of the bernstein mode which is a powerful source of heating in spherical tokamaks. Literature shows the different methods of their coupling. But their unstable regions are a major problem in the coupling. Padoba *et al.* [17] first time demonstrated the conversion from an O-mode to an X-mode by probe measurements of amplitude and phase of the wave field in the conversion region. Cairns *et al.* [18] used sheared magnetic field to calculate the linear conversion of the O-mode to the X-mode. Because electron Bernstein waves are analyzed as possible candidates for heating spherical tokamaks. Ram *et al.* [19] developed a kinetic model for studying the energy flow transfer between the X-mode, the O-mode and the EBW in the mode conversion region in the vicinity of the cold plasma upper hybrid resonance. Sodha *et al.* [20] derived the dispersion relation for modulational instabilities of a Gaussian electromagnetic beam propagating in the two modes: O-mode and X-mode, along the externally applied d.c. magnetic field, in a homogeneous magnetoplasma.

The layout of this paper is as follow. Section 2 gives information about the mathematical model of O-mode and X-mode. This section presents the stability analysis and calculates the maximum growth rate. A brief summary of results and discussions is given in Section 3. Section 4 will conclude the results.

2. Mathematical Model

2.1. The Ordinary Mode (O-Mode)

By using kinetic model, the general dispersion relation for perpendicularly propagating O-mode with $k_\parallel = 0$ in

collionless plasma is as follow [21]

$$
\frac{c^2 k_\perp^2}{\omega^2} = 1 + \frac{2\pi}{\omega} \omega_p^2 \int_{-\infty}^{\infty} p_\parallel^2 \, \mathrm{d}p_\parallel \int_0^\infty \mathrm{d}p_\perp \chi_1 \sum_{n=-\infty}^{\infty} \frac{\left[J_n(z) \right]^2}{(\omega - n\Omega_0)}
$$
$$
- \frac{2\pi}{\omega^2} m \omega_p^2 \int_{-\infty}^{\infty} \mathrm{d}p_\parallel \int_0^\infty p_\perp \mathrm{d}p_\perp \left[\frac{p_\parallel}{p_\perp} \left(\frac{p_\parallel}{m} \frac{\partial f_0}{\partial p_\perp} - \frac{p_\perp}{m} \frac{\partial f_0}{\partial p_\parallel} \right) \right]
$$

(1)

Here $\chi_1 = \dfrac{\partial f_0}{\partial p_\perp}$ and f_0 is distribution function.

The energy anisotropic Heaviside distribution function is [22] [23]

$$
f_0 = \frac{1}{2\pi \hat{p}_\perp} \delta \left(p_\perp - \hat{p}_\perp \right) \frac{1}{2\hat{p}_\parallel} H \left(\hat{p}_\parallel^2 - p_\parallel^2 \right)
$$

(2)

$$
p_{\perp,\parallel}^2 = m T_{\perp,\parallel}
$$

where $T_\perp$ and $T_\parallel$ are the effective temperatures in the perpendicular and parallel directions defined as follows

$$
T_\perp = d^3 p \frac{p_\perp^2}{2m} F \left(p_\perp^2, p_\parallel \right)
$$

$$
T_\parallel = 2 d^3 p \frac{p_\parallel^2}{2m} F \left(p_\perp^2, p_\parallel \right)
$$

and their corresponding integrations yields the results

$$
T_\perp = \frac{p_\perp^2}{2m}, \; T_\parallel = \frac{p_\parallel^2}{3m}
$$

Using Equations (1) and (2), we obtain

$$
\frac{c^2 k_\perp^2}{\omega^2} = 1 - \frac{\omega_p^2}{\omega^2} \left[1 + \sum_{n=1}^{\infty} \frac{\eta_o}{A} \left(\frac{2n^2 \Omega_0^2}{\omega^2 - n^2 \Omega_0^2} \right) \right]
$$

(3)

where

$$
\eta_o = 2 \sum_{n=1}^{\infty} \hat{z} J_n \left(\hat{z} \right) J_n' \left(\hat{z} \right)
$$

$$
\hat{z} = \frac{k_\perp \hat{v}_\perp}{\Omega_0}
$$

$$
A = \frac{T_\perp}{T_\parallel} = \frac{\hat{v}_\perp^2}{\hat{v}_\parallel^2}
$$

For principle harmonic *i.e.*, $n = 1$, we get the following linear dispersion relation

$$
\omega^4 - \left(\Omega_0^2 + c^2 k_\perp^2 + \omega_p^2 \right) \omega^2 + \omega_p^2 \Omega_0^2 \left(\frac{\hat{z}^2}{A\beta_\parallel} + 1 - \frac{\eta_o}{A} \right) = 0
$$

(4)

where $\beta_\parallel = \dfrac{\omega_p^2 v_\parallel^2}{c^2 \Omega_0^2}$.

We note that $\left(\dfrac{\hat{z}^2}{A\beta_\parallel} + 1 - \dfrac{\eta_1}{A} \right) < 0$ is the condition for instability.

However, for higher harmonics, the linear dispersion relation takes the form

$$\frac{\omega^2}{\omega_p^2} - \frac{\hat{z}^2}{A\beta_{\parallel}} = 1 + \sum_{n=1}^{\infty} \frac{\eta_o}{A} \left(\frac{2n^2\Omega_0^2}{\omega^2 - n^2\Omega_0^2} \right) \tag{5}$$

2.2. The Extra-Ordinary Mode (X-Mode)

The general dispersion relation of the X-mode is as

$$\frac{c^2 k_{\perp}^2}{\omega^2} = 1 + \frac{2\pi}{\omega} \omega_p^2 \int_{-\infty}^{\infty} p_{\parallel}^2 \, \mathrm{d}p_{\parallel} \int_0^{\infty} \mathrm{d}p_{\perp} \chi_1 \sum_{n=-\infty}^{\infty} \frac{p_{\perp} J_n'^2(z)}{m(\omega - n\Omega_0)} \tag{6}$$

By using the simple mathematical analysis, the dispersion relation of the X-mode is

$$\frac{c^2 k_{\perp}^2}{\omega^2} = 1 - \frac{\omega_p^2}{\omega^2} \sum_{n=1}^{\infty} \eta_x \left(\frac{2\omega^2}{\omega^2 - n^2\Omega_0^2} \right) \tag{7}$$

In terms of A and $\beta_{\parallel}$, the relation can be expressed as

$$\frac{\omega^2}{\omega_p^2} - \frac{\hat{z}^2}{A\beta_{\parallel}} = \sum_{n=1}^{\infty} \eta_x \left(\frac{2\omega^2}{\omega^2 - n^2\Omega_0^2} \right) \tag{8}$$

where

$$\eta_x = \left[2\hat{z} J_n'(z) J_n''(z) + 2\left[J_n'(z) \right]^2 \right]$$

3. Results and Discussion

In this section we will discuss the stability condition and calculate the growth rate for different combinations of A and $\beta_{\parallel}$.

We first numerically discussed the results obtained for the O-mode from Equation (3). Lee [12] has calculated O-mode for three harmonics with the Maxwellian distribution function and concluded that the mode is stable for the Maxwellian distribution. Ichimaru [24] has discussed the O-mode for higher harmonics with nonlocal effects and confirmed the existence of Azbel-Karner resonance when the wave frequency is multiple of electron cyclotron frequency.

The banded emission is observed in plots of A vs $\hat{z}$ in the case of energy anisotropic Heaviside distribution **Figure 1**. This banded emission strongly agrees with the results of Iqbal *et al.* [10] where the anisotropic Fermi Dirac distribution function was used. The wave provides a wide range of stable and unstable regions.

In **Figure 1**, the relation of $\beta_{\parallel}$ and anisotropy A is plotted, it provides a marginal threshold value. The dotted curve shows that $\frac{\hat{z}^2}{A\beta_{\parallel}} + 1 = \frac{\eta_O}{A}$, this curve plays the role of threshold value between stable and unstable O-mode. Below the dotted curve the condition $\frac{\hat{z}^2}{A\beta_{\parallel}} + 1 < \frac{\eta_O}{A}$ satisfies and mode is unstable which is presented by dashed curve. Above that dotted curve the condition is $\frac{\hat{z}^2}{A\beta_{\parallel}} + 1 > \frac{\eta_O}{A}$, it means that there is a stable region *i.e.*, the solid curve. The comparison of plots defines that for small $\hat{z}^2$ the $\beta_{\parallel}$ contains large value, this is the region where $\beta_{\parallel}$ is large enough to provide a growth rate much larger than the oscillatory frequency $\omega_r \ll \omega_i$ so these results strongly agree with the environment *i.e.*, solar wind. For large anisotropy, $T_{\parallel}/T_{\perp} > 10$, or for large $\beta_{\parallel} > 10$, the O-mode instability is faster than the firehose instability. Larger values of $\beta_{\parallel}$ means low magnetic fields or more dense and hotter plasma, these conditions can come across at different altitudes in the solar wind regime.

In series of **Figures 2-5**, growth rates of higher harmonics have been plotted. For analytical threshold we consider complex form $\omega^2 = (\omega_r + i\omega_i)^2$, in plots the solid lines represent the ω_r and dashed shows the ω_i, where $\beta_{\parallel} = 4.0$ for **Figures 2-5**.
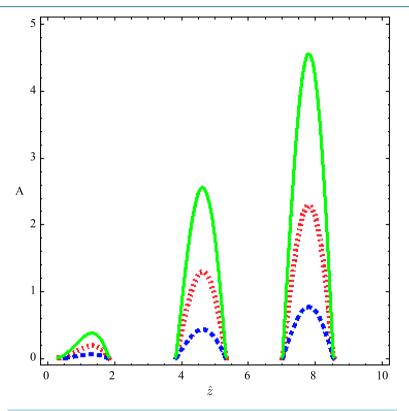
Figure 1. Marginal stability condition.

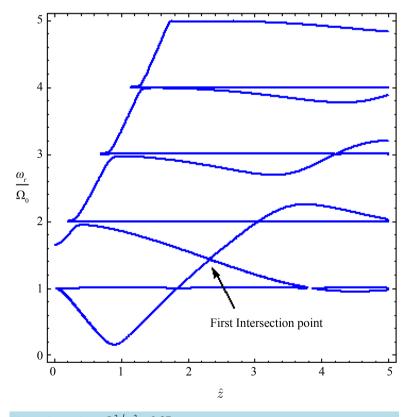**Figure 2.** $A = 0.1$, $\Omega_0^2 / \omega_p^2 = 0.37$.

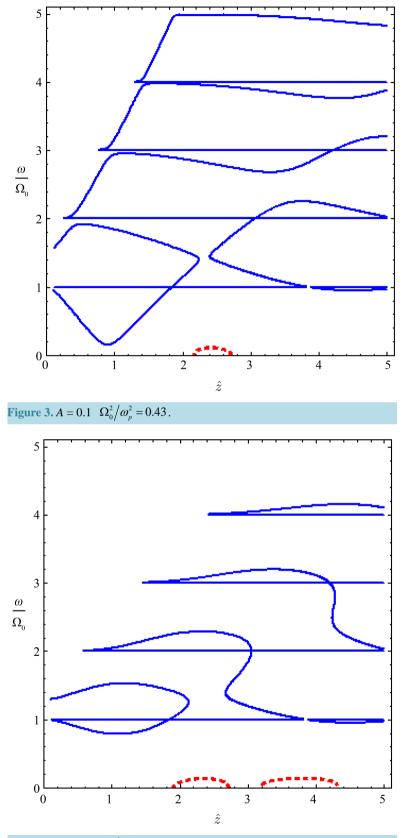**Figure 3.** $A = 0.1$ $\Omega_0^2/\omega_p^2 = 0.43$.

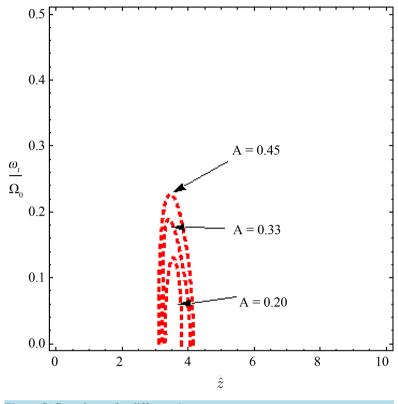**Figure 4.** $A = 0.6$ $\Omega_0^2/\omega_p^2 = 0.9$.

Figure 5. Growth rate for different A.

In **Figure 2**, there is a stable form of O-mode but at $A = 0.1$ and $\Omega_0^2/\omega_p^2 = 0.37$ the harmonics start to intersect with each other.

Figures 3-5 show the real part of dispersion relation and dependence of O-mode on magnetic field. As we increase values of magnetic field, $\Omega_0^2/\omega_p^2 = 0.43$ it becomes unstable and the first unphysical state generates as in **Figure 3**. These results also satisfy the marginal instability condition as discussed earlier numerically. In above plots, noticeable thing is the value of $A = 0.1$. The parallel streaming is dominating in O-mode and playing a role to destabilize the wave. The plasma beta is greater than one so these effects satisfy the high plasma beta regimes.

On further increasing the magnetic field, unstable regions are obtained and at $\Omega_0^2/\omega_p^2 = 0.6$ and $A = 0.9$, the wave becomes totally unstable as in **Figure 4**.

The growth rate shows that parallel streaming responsible to grow the wave. The complex part of the dispersion relation tells that the wave is growing in the gaps. **Figure 5** shows the growing parts of the first two gaps.

The O-mode instability divides in two branches for complex ω. First branch is oscillatory when $\omega_i = 0$ and second branch is aperiodic or purely growing when $\omega_r = 0$ as in **Figure 6**. Further increasing the value of parallel streaming, the aperiodic branch is obtained. For oscillatory branch the magnetic field plays a role to destabilize the wave and increase the growth of the wave.

For second branch, which is aperiodic or purely growing, the trend totally reverses . The growth rate increases with the decreasing value of A. The result proves that the anisotropy stabilizes the purely growing part. **Figure 7** shows the increasing growth rate of aperiodic mode with decreasing value of A. The noticeable thing is that this part also satisfies the condition of the firehose instability *i.e.*, $T_\parallel > T_\perp$ and $\beta_\parallel > 1$. The purely growing wave is also called non-propagating firehose instability [25] The study of variation of anisotropy tells us that with the increasing value of A, the growth rate is also increases that means by increasing value of A destabilizes the wave. When $T_\parallel > T_\perp$ and $\beta_\parallel > 1$, then wave becomes more unstable this result proves that O-mode instability satisfies the condition of the firehose instability.

For number of harmonics, the X-mode is also unstable but for this mode perpendicular temperature is
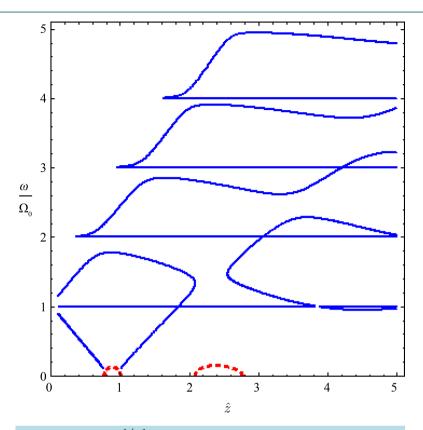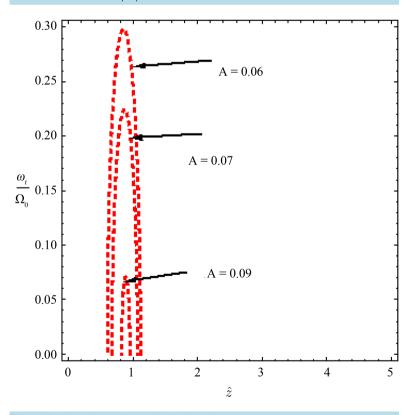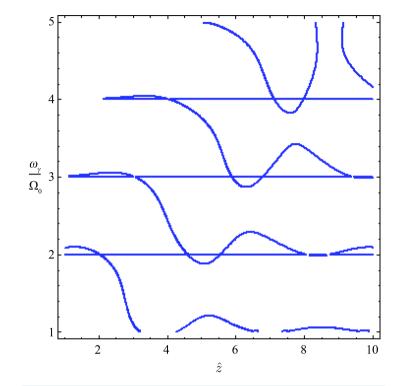
Figure 6. $A = 0.09$ $\Omega_0^2/\omega_p^2 = 0.9$.

Figure 7. Growth rate for aperiodic branch.

dominating. The wave becomes unstable for larger value of *A*. In **Figure 8** when *A* = 6.5, the wave is stable. But after that when *A* = 6.96, the harmonics overlap each other and wave starts to be unstable as in **Figure 9**.

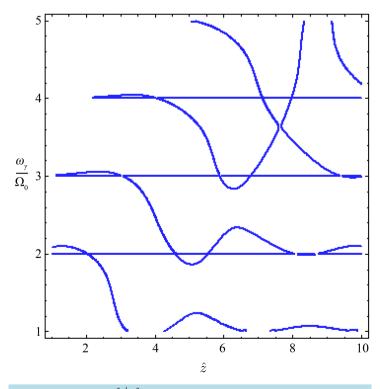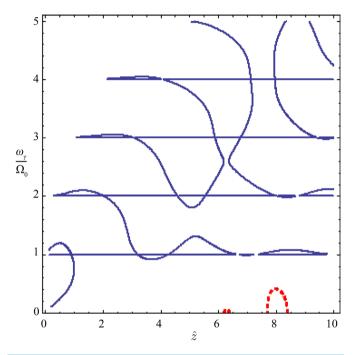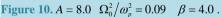**Figure 8.** $A = 6.5$ $\Omega_0^2/\omega_p^2 = 0.09$ $\beta = 4.0$.

Figure 9. $A = 6.69$ Ω_0^2/ω_p^2 $\beta = 4.0$.

On further increasing the value of A the mode becomes more unstable as in **Figure 10** the value of A is 8 and $\Omega_0^2/\omega_p^2 = 0.09$. The solid curves show the real part of the wave and dashed curves show the growth of the said wave. The increasing value of A shows that in X-mode instability perpendicular streaming is dominating. At $A = 11$, it becomes totally unstable **Figure 11**.

Figure 12 discusses that the growth rate increases with the increasing value of anisotropy. Anisotropy de-stabilizes the X-mode, the X-mode follows the same trend as that of the O-mode.
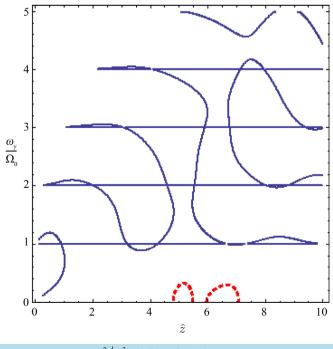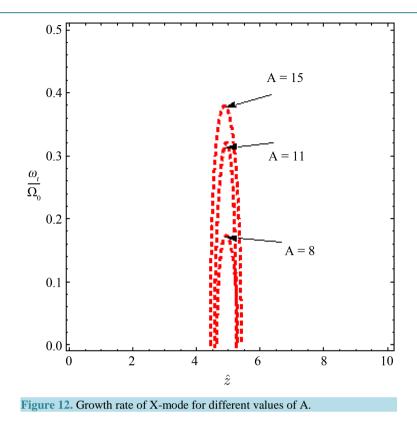

Figure 10. $A = 8.0$ $\Omega_0^2/\omega_p^2 = 0.09$ $\beta = 4.0$.

Figure 11. $A = 11$ $\Omega_0^2/\omega_p^2 = 0.09$ $\beta = 4.0$.

Figure 12. Growth rate of X-mode for different values of A.

4. Conclusion

O-mode instability, for principle harmonic, depends upon the magnetic field even it is weaker. The instability generates due to temperature anisotropy and free energy of anisotropy converted in the magnetic induction which is the reason of growing wave. The growth rate varies directly with the value of ratio of anisotropy. Here we have calculated the marginal threshold condition in form of plasma parameters A and $\beta_\parallel$ for principle harmonic. For higher harmonics, oscillatory branch satisfies the statement and purely growing part inverts the condition. It varies inversely with the anisotropy. The oscillatory and purely growing mode both satisfies the conditions of firehose instability *i.e.*, $T_\parallel > T_\perp$ and $\beta_\parallel > 1$ as $B_0 \parallel E$ in O-mode. The stability analysis of the X-mode tells that perpendicular temperature is dominating. The mode is unstable for $T_\perp > T_\parallel$, according to geometry of the X-mode that is $B_0 \perp E$. Coupling of these two modes converts them into the Bernstein mode which is responsible of heating effects in tokamak. The O-X conversion is the method of achieving the Bernstein mode.

Acknowledgements

References

[1]   Ono, M., *et al.*, (2004) *Nuclear Fusion*, **44**, 452. http://dx.doi.org/10.1088/0029-5515/44/3/011

[2]   Akers, R.-J., *et al.*, (2002) *Physics of Plasmas*, **9**, 3919. http://dx.doi.org/10.1063/1.1490928

[3]   Whaley, D.R., *et al.* (1992) *Nuclear Fusion*, **32**, 757. http://dx.doi.org/10.1088/0029-5515/32/5/I04

[4]   Hamasaki, S. (1968) *Physics of Fluids*, **11**, 12.

[5]   Hamasaki, S. (1968) *Physics of Fluids*, **6**, 11.

[6]   Lee, K.F. (1969) *Physics Review*, **1**, 181.

[7]   Bornatici, M. and Lee, K.F. (1971) *Physics Fluids*, **13**, 42.

[8]   Shivamoggi, B.K. (1982) *Astrophysics and Space Science*, **82**, 481-483. http://dx.doi.org/10.1007/BF00651455

[9]   Ibschar, D., Lazar, M. and Schlickeiser, R. (2012) *Physics of Plasmas*, **19**, 072116. http://dx.doi.org/10.1063/1.4736992

[10] Iqbal, Z., Hussain, A., Murtaza, G. and Tsintsadze, N.L. (2014) *Physics of Plasmas*, **21**, 032128. http://dx.doi.org/10.1063/1.4870007

[11] Hadi, F., Yoon, P.H. and Qamar, A. (2015) *Physics of Plasmas*, **22**, 022112. http://dx.doi.org/10.1063/1.4907657

[12] Lazar, M., Schlickeiser, R., Poedts, S., Stockem, A. and Van, S. (2014) http://arxiv.org/abs/1411.1508

[13] Vafin, S., Schlickeiser, R. and Yoon, P.H. (2014) *Physics of Plasmas*, **21**, 104504. http://dx.doi.org/10.1063/1.4897373

[14] Farrell, W.M. (2001) *Journal of Geophysical Research*: *Space Physics*, **106**, 15701-15709. http://dx.doi.org/10.1029/2000JA000156

[15] Colpitts, C.A., Cattell, C.A., Kozyra, J.U. and Parrot, M. (2012) *Journal of Geophysical Research*: *Space Physics*, **117**. http://dx.doi.org/10.1029/2011JA017329

[16] LaBelle, J., Ruppert, D.R. and Treumann, R.A. (1999) *Journal of Geophysical Research*, **104**, 293-303. http://dx.doi.org/10.1029/1998JA900050

[17] Podoba, Y.Y., Laqua, H.P., Warr, G.B., Schubert, M., Otte, M., Marsen, S. and Wagner, F. (2007) *Physical Review Letters*, **98**, 255003. http://dx.doi.org/10.1103/PhysRevLett.98.255003

[18] Cairns, R.A. and Lashmore-Daviesa, C.N. (2000) *Physics of Plasmas*, **7**, 4126-4134.

[19] Ram, A.K., Bers, A. and Lashmore-Davies, C.N. (2002) *Physics of Plasmas*, **9**, 409-418. http://dx.doi.org/10.1063/1.1429634

[20] Sodha, M.S., Sharma, R.P., Maheshwari, K.P. and Kaushik, S.C. (1977) *Plasma Physics*, **20**, 585. http://dx.doi.org/10.1088/0032-1028/20/6/009

[21] Bashir, M.F. and Murtaza, G. (2012) *Brazilian Journal of Physics*, **42**, 487-504.

[22] Yoon, P.H. and Davidson, R.C. (1987) *Physical Review A*, **35**, 2718-2721.

[23] Bashir, M.F., Noreen, N., Murtaza, G. and Yoon, P.H. (2014) *Plasma Physics and Controlled Fusion*, **56**, Article ID: 055009.

[24] Ichimaru, S. (1973) Basic Principles of Plasma Physics: A Statistical Approach. Addison-Wesley Publishing Company, New York, 104.

[25] Lazar, M., Poedts, S., Schlickeiser, R. and Ibscher, D. (2014) *Solar Physics*, **289**, 369-378. http://arxiv.org/abs/1307.0768